

Optimization of sulfamethoxazole degradation by TiO₂/hydroxyapatite composite under ultraviolet irradiation using response surface methodology

Suk Young Chun*, Sang Woo An**, Si Jin Lee***, Ji Tae Kim*, and Soon Woong Chang*[†]

*Department of Environmental Energy Systems Engineering, Kyonggi University, Suwon 443-760, Korea

**Department of Civil and Environmental Engineering, Hanyang University, Seoul 133-791, Korea

***Korea Environment Corporation, Incheon 404-708, Korea

(Received 22 September 2013 • accepted 22 January 2014)

Abstract—A titanium dioxide/hydroxyapatite/ultraviolet (TiO₂/HAP/UV-A) system was used to remove sulfamethoxazole (SMX) from water in a second-order response surface methodology (RSM) experiment with a three-level Box-Behnken design (BBD) for optimization. The effects of both the primary and secondary interaction effects of three photocatalytic reaction variables were examined: the concentration of SMX (X_1), dose of TiO₂/HAP composite (X_2), and UV intensity (X_3). The UV intensity and TiO₂/HAP dose significantly influence the SMX and total organic carbon (TOC) removal ($p < 0.001$). However, the SMX and TOC removal are enhanced with increasing TiO₂/HAP dose up to certain levels, and further increases in the TiO₂/HAP dose result in adverse effects due to hydroxyl radical scavenging at higher catalyst concentrations. Complete removal of SMX was achieved upon UV-A irradiation for 180 min. Under optimal conditions, 51.2% of the TOC was removed, indicating the formation of intermediate products during SMX degradation. The optimal ratio of SMX (mg L⁻¹) to TiO₂/HAP (g L⁻¹) to UV (W/L) was 5.4145 mg L⁻¹ to 1.4351 g L⁻¹ to 18 W for both SMX and TOC removal. By comparison with actual applications, the experimental results were found to be in good agreement with the model's predictions, with mean results for SMX and TOC removal of 99.89% and 51.01%, respectively.

Keywords: TiO₂/HAP Composite, Sulfamethoxazole, Response Surface Methodology, Photocatalysis, Optimization

INTRODUCTION

Low concentrations of antibiotics have been observed in aquatic environments because of their continuous discharge from wastewater treatment plants (WWTPs), which has led to various problems such as the emergence of antibiotic-resistant bacteria [1-3]. Sulfamethoxazole (SMX, C₁₀H₁₁N₃O₂S) is a synthetic antibiotic that belongs to the group of sulfonamide antibiotics. It is commonly used for the treatment of bronchitis and urinary tract infections as well as in veterinary medicine [1].

SMX is a nondegradable pollutant in aqueous media that might not be treatable with traditional biological treatment systems because of its antibacterial nature [4]. It is believed that SMX is not readily biodegradable in WWTPs, although other studies concluded that the SMX has the potential to be biodegraded given a very long residence time [5]. Alexy et al. [4] also reported the up to 27% of the SMX biodegraded after 28 days. Thus, the continuous discharge of SMX into the ecosystem could cause adverse effects, including the development of more harmful bacteria with enhanced antibiotic resistance [6].

In general, advanced oxidation processes (AOPs) act through the formation of radicals that react with and destroy the target compounds. The common AOPs include ozone, UV/ozone, and UV/H₂O₂ treatments, which involve oxidation by the generated hydroxyl radicals. The UV-A/TiO₂ processes are dependent on several vari-

ables, including the initial concentration, catalyst phase identity and dose, electron acceptor identity, and the presence of non-target water constituents [7]. For example, Degussa P-25 TiO₂ has been most often applied to degrade SMX, and some studies have reported that biomaterials can enhance the photocatalytic activity of TiO₂. However, there are no reports on the enhancement of the potential of TiO₂ for SMX degradation by biomaterials as hydroxyapatite (HAP). The synergistic effect of HAP with TiO₂ should, without high cost, lower the degree of the toxicity and antimicrobial activity of SMX [8]. HAP is a biomaterial generally used as an adsorbent, and also exhibits good biocompatibility [8,9]. Thus, the TiO₂/HAP composite was used for the photocatalytic degradation of SMX, and the effects of the TiO₂/HAP molar ratio and of the use of HAP-supported TiO₂ under UV-A irradiation were examined to determine the optimum conditions for SMX and TOC removal.

For the statistical aspect of this approach, the response surface methodology (RSM) was used to find the main and interaction effects and to optimize the SMX and TOC removal process. RSM is a well-verified tool for process optimization. It is a collection of mathematical and statistical techniques for analyzing the effects of several independent variables and employs a low-order polynomial equation in a predetermined region of variables, which will later be analyzed to locate the optimum values of the independent variables for process optimization [10]. The kinetics of the SMX degradation was also examined to determine the effects of various catalysts and to compare the kinetics results with the RSM results to provide a more robust approach to SMX degradation.

The objective of this study is to evaluate the enhancement in the photocatalytic activity of TiO₂/HAP over that of Degussa P25 TiO₂

[†]To whom correspondence should be addressed.

E-mail: swchang@kgu.ac.kr

Copyright by The Korean Institute of Chemical Engineers.

and to determine the optimal experimental conditions for photocatalytic SMX degradation in the TiO₂/HAP/UV-A process by using RSM to examine both single and combined effects of three independent variables: SMX concentration, TiO₂/HAP dose, and UV intensity.

MATERIALS AND METHODS

1. Chemicals and Analytical Methods

Analytical-grade SMX (C₁₀H₁₁N₃O₃S, >99%) was obtained from Sigma-Aldrich, Canada. Aqueous stock solution (100 mg L⁻¹ SMX) was prepared with deionized water obtained from a Milli-Q system (Waters, USA) and was kept at 4 °C in the dark until the time of treatment. Commercial TiO₂ Degussa P25 (70% anatase and 30% rutile, Evonik Degussa Canada Inc.) and HAP (Sigma-Aldrich, Canada) were used as catalysts on their own and as the materials for the TiO₂/HAP composite catalyst. HPLC-grade methanol, acetonitrile, and isopropanol were purchased from Fisher Scientific, Canada, and 95% ethanol was purchased from Commercial Alcohols (Boucherville, Quebec, Canada). The SMX concentration was measured by a high-performance liquid chromatograph (Agilent 1100series HPLC, USA) equipped with an XTerra MS C18 column (2.5 μm, 2.1 mm×50 mm), and the analytical mode was the selected ion monitoring (SIM) mode. The mineralization of SMX was analyzed in terms of the TOC using a TOC analyzer (Shimadzu TOC-V CSN).

2. Synthesis

TiO₂ of Degussa P-25 (70% anatase and 30% rutile) and HAP (Sigma-Aldrich, Canada) were used as catalyst with an average particle size of 30 nm and BET surface area of above 50 m² g⁻¹. The TiO₂/HAP composite was prepared by sol-gel method using 2-propanol, TiO₂ and HAP as the starting materials and HNO₃ solution as the pH adjusting agent. Initially a 10 mM suspension of TiO₂ and 1 mM HAP were prepared and stirred using magnetic stirrer. Then, about 10 mL of 2-propanol solution was added dropwise to the TiO₂ suspension. Following that, the pH of mixture suspension was adjusted to 1.5 by adding HNO₃ solution. After thoroughly mixing the reactants, the mixed solution was stirred at room temperature. The prepared suspension was evaporated for 2 hr using rotary evaporator. The prepared powder of TiO₂/HAP composite was formed by dry ball milling and calcined in an oven at 500 °C and for 2 hrs.

3. Reactors and Procedure

The following experimental conditions were kept constant throughout this work: 1 L of total volume, 10 mg L⁻¹ initial SMX concentration, and 1,000 mg L⁻¹ of added TiO₂ (Degussa, P-25) or TiO₂/HAP composite. This concentration of SMX, although considerably greater than those typically monitored in the field or the environment, was chosen to evaluate the process efficiency within a certain time scale and for accurate analysis of the SMX photodegradation and mineralization with the analytical techniques employed in this study. The batch reactor maintains thermostatic conditions and consists of a 1.5 L quartz reservoir (inner diameter 11 cm; height 23 cm) equipped with three lamps (length 22.5 cm) placed in its center (Philips TL 6W/05, UV-A), with nominal power of 6 W each, that emit radiation between 350 and 400 nm with a maximum at 365 nm. The reservoir (1 L) was loaded with 10 mg L⁻¹ SMX solution that was recirculated during the UV-A irradiation time. At given irradiation time intervals, 10 mL of the reacted solution was taken from the sampling port of the reactor and centrifuged at 12,000 rpm to

Table 1. Experimental ranges and actual values of independent variables

Coded levels (x _i)	Actual level			
	X ₁ (mg L ⁻¹) ^a	X ₂ (g L ⁻¹) ^b	X ₃ (W L ⁻¹) ^c	
Max. level	+1	15	1.5	18
Central level	0	10	1.0	12
Min. level	-1	5	0.5	6

^aConcentration of SMX

^bCatalyst dose

^cUV intensity

remove the catalyst particles.

4. Box-Behnken Design

A Box-Behnken design (BBD) was used to determine the optimal conditions with a rotatable experimental plan. The variable combinations are at the midpoints of the edges and at the center of the variable space [11,12]. For the photocatalytic process, the significant variables, namely, the concentration of the target compound (SMX), catalyst dose, and UV intensity, were chosen as the independent variables and designated as X₁–X₃, respectively. The SMX concentration (X₁) ranged from 5 to 15 mg L⁻¹, the TiO₂/HAP dose (X₂) ranged from 0.5 to 1.5 g L⁻¹, and the UV intensity (X₃) ranged from 6 to 18 W L⁻¹, as shown in Table 1. The actual values of the independent variables (X_i) were coded as x_i according to Eq. (1) by setting the lowest values as -1 and the highest values as +1:

$$x_i = (X_i - X_0) / \Delta X \quad (1)$$

In Eq. (1), x_i is the dimensionless value of an independent variable, X_i represents the real value of the independent variable, X₀ is the real value of the independent variable at the center point, and ΔX_i is the step change [11,12]. The independent variables for the BBD experiments were set based on the initial values at the center points. The three independent variables (X₁, X₂, and X₃) were used to fit the general model of Eq. (2) and to obtain optimal conditions for the response (Y_i).

$$Y = \beta_0 + \sum_i \beta_i x_i + \sum_i \beta_{ii} x_i^2 + \sum_{j>i} \beta_{ij} x_i x_j \quad (2)$$

In addition, the mathematical relationship describing the response can be approximated by the following quadratic (second-order) polynomial equation, Eq. (3):

$$Y = \beta_0 + \beta_1 x_1 + \beta_2 x_2 + \beta_3 x_3 + \beta_{11} x_1^2 + \beta_{22} x_2^2 + \beta_{33} x_3^2 + \beta_{12} x_1 x_2 + \beta_{13} x_1 x_3 + \beta_{23} x_2 x_3 \quad (3)$$

The response values (Y_i) were chosen to be the SMX (Y₁) and TOC removal (Y₂). Experimental data analysis was performed using the Minitab 14.1 (USA) software, and the statistical analysis was achieved by regression analysis and the analysis of variance (ANOVA) test at a 95% confidence level.

RESULTS AND DISCUSSION

1. Characterization of TiO₂/HAP Composite

An X-ray diffractometer (XRD, X'Pert Powder, Netherlands), a scanning electron microscope (SEM, FEI Quanta 200) and EDX (Energy dispersive X-ray spectroscopy) were used to characterize the crystal structure and morphology, respectively, of the TiO₂/HAP

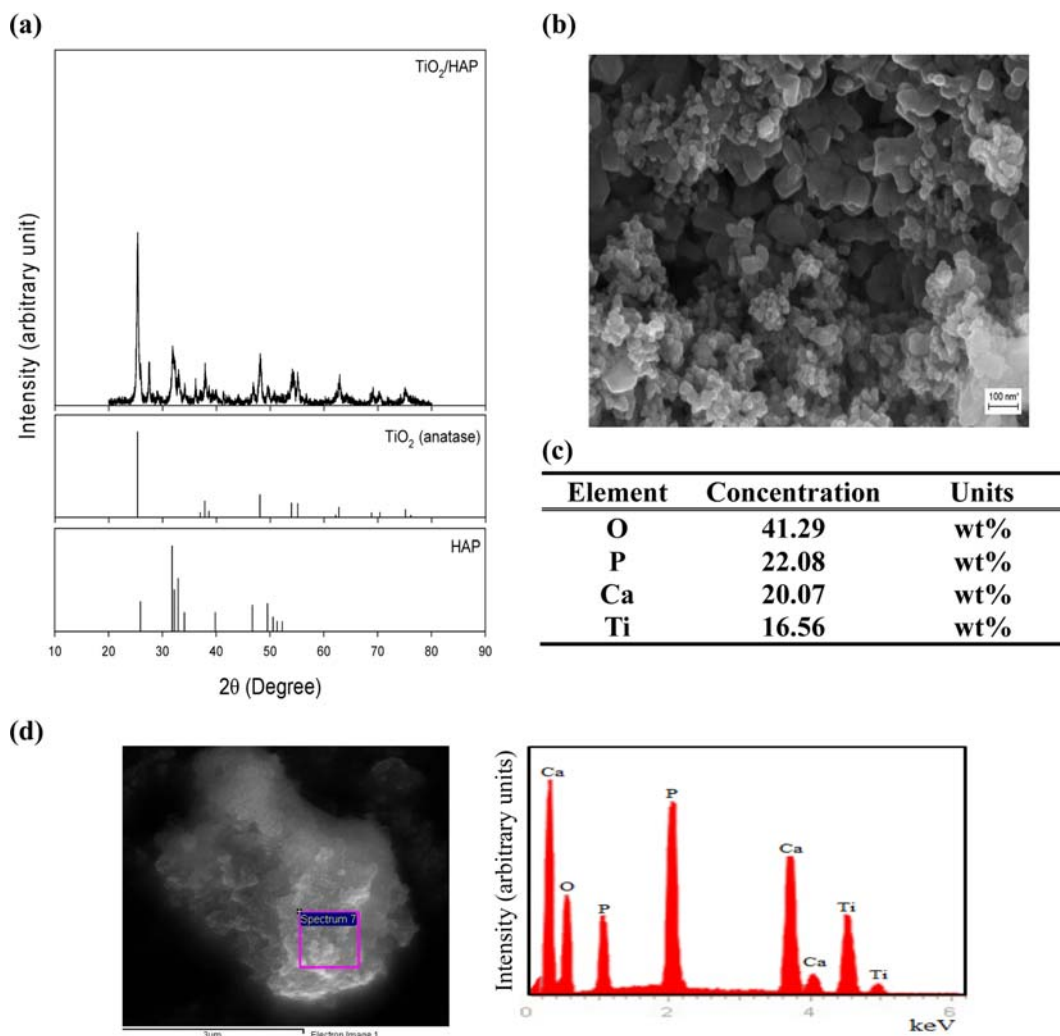


Fig. 1. Characterization results for the TiO_2/HAP composite fabricated by heat treatment at 500°C for 120 min: XRD pattern (a), SEM image (b) and EDX analysis of TiO_2/HAP composite (c) and (d).

composite. As shown in Fig. 1(a), the crystallinity of the prepared HAP is confirmed by reflections observed at 2θ values of 26.1° , 32.4° , 33.2° , 34.1° , 39.8° , 47.1° , and 49.6° , and anatase-phase TiO_2 is revealed by the peaks at 2θ values of 25.4° , 38.0° , 48.1° , 53.9° , and 55.3° .

The characteristic diffraction peaks of the TiO_2/HAP composite confirmed that the main constituents were TiO_2 (anatase) and HAP, which is similar to the result reported previously [13]. In the XRD patterns, there were diffraction peaks corresponding to the anatase phase, while the HAP phase of TiO_2/HAP was also detected, indicating that the photocatalytic activity and adsorption occurred for both the anatase and HAP phases.

Fig. 1(b) shows SEM photographs of the top surface of the TiO_2/HAP composite. The grayish surface obtained after HAP loading using the sol-gel method reveals that the TiO_2 is codoped with HAP. In addition, the surface of the TiO_2/HAP composite has a regular sphere morphology. These XRD and SEM results agree with those of Wang et al. [14], who reported the enhanced photocatalytic activity of the TiO_2/HAP composite. However, the particle size of our TiO_2/HAP structure was smaller than that in Wang's [14] SEM image of their TiO_2/HAP composite. However, the synthetic procedure

for TiO_2/HAP was similar to that used to produce the codoped HAP, so the molar ratio of TiO_2 to HAP and the heat treatment conditions seem to be the reasons for the different structure sizes.

The results of measurements of TiO_2/HAP composition by EDX analysis are presented in Fig. 1(c) and (d). They show the homogeneity of composition by measuring concentration ratio of Ca, P, O and Ti from various parts of TiO_2/HAP composite. Fig. 1(d) summarizes the results of contents of TiO_2 and HAP in TiO_2/HAP composite.

2. Comparison of SMX Removal

The SMX degradation was carried out under both UV-A irradiation and dark conditions with as-prepared Degussa P25 TiO_2 , HAP, and a TiO_2/HAP composite to compare the adsorption and photocatalytic activity. And the experimental conditions such as 1 L total volume, 10 mg L^{-1} of SMX contact with 1 g L^{-1} of each catalysts addition amount and the temperature was maintained at $25\pm 1^\circ\text{C}$ and good mixing was provided using a stirrer at 100 rpm. The pH was adjusted to near-neutral pH ($\text{pH } 6.5\pm 0.1$). And at given adsorption and irradiation time intervals (adsorption=5, 10, 15, 20, 25, 30, 45 and 60 min, irradiation=60, 65, 70, 75, 90, 120, 180, 240 and 300 min) 10 mL of the reacted solution was sampled. The results obtained under dark conditions (for 60 min of stirring) were used

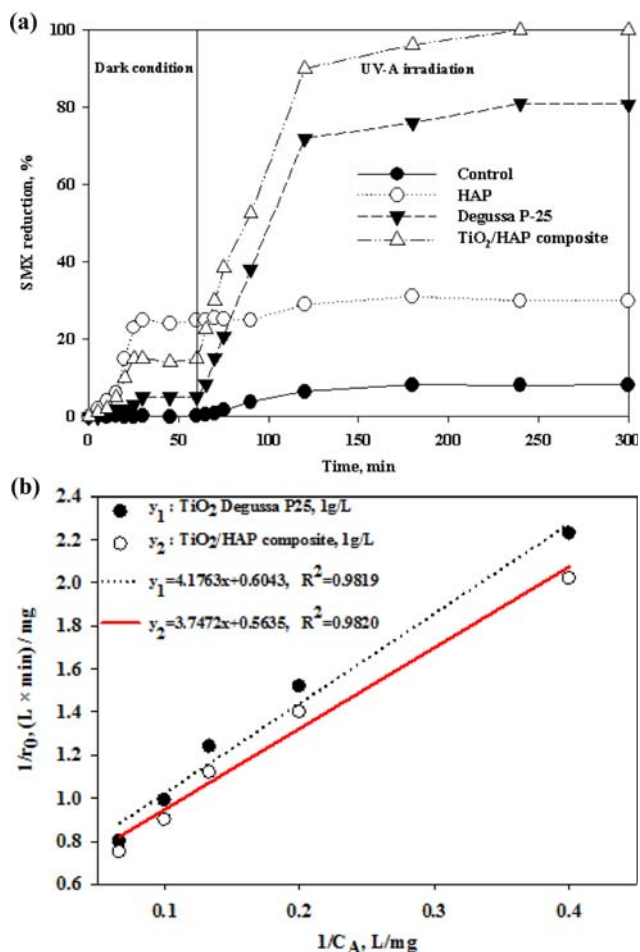


Fig. 2. Comparison of various catalysts for (a) SMX degradation during 60 min under dark conditions and during 240 min of UV-A irradiation and (b) the Langmuir-Hinshelwood kinetic model of TiO₂ Degussa P25 and TiO₂/HAP composite.

to determine the amount of SMX removed by adsorption. Xu et al. [15] reported that the interaction between SMX molecules and TiO₂-based photocatalytic materials is affected by both of the surface properties and the structure of the target compounds [15].

As shown in Fig. 2(a), the results obtained for SMX adsorption by Degussa P25 TiO₂, HAP, and the TiO₂/HAP composite under dark conditions demonstrate that SMX did not adsorb appreciably over the Degussa P-25 TiO₂ (less than 5% SMX removal for 1 h batch experiments), but the TiO₂/HAP composite and HAP adsorb nearly 15% and 25% of the SMX, respectively. The higher adsorption capacity of HAP leads to a relatively high adsorption rate for organic pollutants, which allows the adsorption equilibrium to be reached in a short time [22,23].

Fig. 2(a) also shows the adsorption activities of various catalysts after 60 min in the dark. For the HAP sample, the adsorption capacity was higher than that for all the other samples, but still only 25% SMX conversion was observed in 60 min. This is because the HAP is capable of only adsorption, rather than decomposition, of the SMX, and once saturation is reached, the adsorption activity weakens rapidly.

In particular, the adsorption capacity of the TiO₂/HAP composite (about 15%) was higher than that of Degussa P-25 TiO₂ (below 5%). Thus, the adsorption capacity of the composite seems to have

been increased by the HAP loading. These results are in good agreement with those of Tsukada et al. [8] and Ma et al. [16], who reported that the adsorption capacities of various catalysts (including TiO₂ Degussa P25) were enhanced by HAP loading.

The SMX degradation can be explained in terms of two steps, adsorption and photocatalytic oxidation, according to the Langmuir-Hinshelwood kinetic model (Eq. (4)) [17,18]. The rate constant for photolysis was also observed, but it was not studied here since the higher reaction rates for adsorption and photocatalysis are considered to lead to the more rapid SMX removal.

$$r_0 = k_r \frac{KC_A}{1 + KC_A} \Leftrightarrow \frac{1}{r_0} = \frac{1}{k_r} \frac{1}{KC_A} + \frac{1}{k_r} \quad (4)$$

In Eq. (4), r_0 is the initial reaction rate for SMX photocatalytic degradation, C_A is the initial SMX concentration, K is the adsorption constant of SMX over the catalyst, and k_r is the intrinsic reaction rate constant. Fig. 2(b) presents the kinetic experiments carried out using various initial concentrations of SMX (2.5, 5, 7.5, 10 and 15 mg L⁻¹) with irradiation time. From these experimental results, the values of K for SMX degradation by adsorption and photocatalysis with various catalysts are summarized in Table 2. The k_r and K values calculated according to Eq. (4) from the slope of the straight line and from the intercept.

The TiO₂/HAP composite has a higher rate constant than Degussa P25 TiO₂. The photocatalytic activity (k_r) and adsorption capacity (K) were enhanced by the added HAP, which seems to have a synergistic effect with TiO₂, as evidenced by the higher k_r (k_r term) for the composite than for any other catalyst. These results can explain the enhanced rate for degradation of SMX by the TiO₂/HAP composite as compared to that for the Degussa P-25 TiO₂ catalyst. This enhancement is the result of rapid SMX degradation at the surface of TiO₂/HAP composite by adsorption ($k_{adsorption}=0.1504$) and photocatalysis ($k_{photocatalysis}=1.7746$). On the other hand, the Degussa P-25 generated radical species, as shown in Table 2 ($k_{photocatalysis}=1.6548$), and the chance of contact with SMX ($k_{adsorption}=0.1447$) was also lower than for the TiO₂/HAP composite. Therefore, the TiO₂/HAP composite has more photocatalytic activity than Degussa P25 TiO₂ ($k_rK=0.2394$), with a rate constant higher by a factor of 1.1149 (TiO₂/HAP composite $k_rK=0.2669$). Wang et al. [14] and Liu et al. [24] reported that HAP has excellent biocompatibility when combined with TiO₂, at least to a certain extent. This good biocompatibility and the previously discussed relatively high catalytic reactivity of TiO₂/HAP results in the enhanced photocatalytic degradation rate shown in Table 2. Thus, the TiO₂/HAP composite can be considered an effective alternative to Degussa P25 TiO₂ for SMX degradation.

Fig. 2(a) also shows that the SMX degradation potential of the TiO₂/HAP composite is considerably higher than those of the Degussa P25 TiO₂ and HAP samples, leading to nearly complete SMX conversion after 180 min of UV-A irradiation. In contrast, the conver-

Table 2. Apparent first-order rate constant for the adsorption and photocatalysis

Term	Degussa P-25 TiO ₂	TiO ₂ /HAP composite
k_rK ($k_{photocatalysis+adsorption}$)	0.2394	0.2669
K ($k_{adsorption}$)	0.1447	0.1504
k_r ($k_{photocatalysis}$)	1.6548	1.7746

sion of SMX by Degussa P25 TiO₂ did not exceed 80% after 240 min of UV-A irradiation time. Nasuhoglu et al. [1] also reported that Degussa P25 TiO₂ completely degraded the SMX under UV-C irradiation. However, UV-C irradiation is generally more effective than UV-A irradiation for degrading SMX by photolysis alone (UV-A was used in this study, and only 8% of the SMX was degraded by photolysis). Thus, complete SMX decomposition under UV-A irradiation was only obtained from the TiO₂/HAP composite, which has higher photocatalytic activity than the Degussa P25 TiO₂ catalyst. At the same time, a control experiment was conducted to examine the photolysis of SMX under UV-A conditions. The photolysis of SMX is favored in the absence of catalyst, and about 8% conversion was reached after 240 min of UV-A irradiation. In general, the UV-A/TiO₂ system yields less photocatalytic degradation than the UV-C/TiO₂ or UV-C/H₂O₂ systems. However, the UV-A/TiO₂ system has advantages in areas related to the cost, such as the consumption of electricity. Furthermore, the TiO₂/HAP composite has enhanced photocatalytic activity for SMX removal, which is important for applications in wastewater treatment or the production of drinking water.

3. Application of Box-Behnken Design

The BBD (Table 3) allows mathematical equations relating each response (Y_i) to the independent variables (X_i) to be developed [12]. Table 3 shows the BBD used in the present study. These experimental designs were used to optimize the UV-A/TiO₂/HAP process in accordance with the response surface. The three design factors (independent variables X_i) involved in the BBD were each set to three different levels: the minimum point, center point, and maximum point. A total of 15 experiments were conducted at different concentrations of SMX (X_1), TiO₂/HAP doses (X_2), and irradiation intensities (X_3). The BBD and the results of these 15 experimental runs are shown in Table 3.

Table 4 shows the analysis of variance (ANOVA) for the regression parameters of the predicted response models for SMX removal (Y_1 , %) and TOC removal (Y_2 , %). As shown in Table 4, the results revealed that the regression model was significant at the 95% confidence level ($P < 0.05$). All the linear, quadratic, and interaction parameters were also significant for both SMX and TOC removal, with p values less than 0.05.

All functions of X_1 , X_2 , and X_3 were calculated as sums of a con-

Table 3. Experimental design for SMX degradation using BBD

Run order	Coded factor			Uncoded factor			SMX removal, %	TOC removal, %
	x_1	x_2	x_3	X_1	X_2	X_3	Y_1	Y_2
1	-1	0	1	5	1.5	18	97.2	47.2
2	1	-1	0	15	1	12	91.6	41.6
3	1	1	0	15	2	12	96.3	48.3
4	0	-1	1	10	1	18	94.7	44.7
5	0	0	0	10	1.5	12	95.4	45.4
6	0	0	0	10	1.5	12	95.6	45.6
7	1	0	-1	15	1.5	6	92.1	42.1
8	0	1	-1	10	2	6	93.4	43.4
9	-1	1	0	5	2	12	96.0	46.0
10	0	-1	-1	10	1	6	91.0	41.0
11	0	1	1	10	2	18	100	51.4
12	-1	-1	0	5	1.5	12	91.3	41.8
13	-1	0	-1	5	1.5	6	90.2	38.7
14	1	0	1	15	1.5	18	96.2	46.2
15	0	0	0	10	1.5	12	95.8	45.8

stant, first-order effects, second-order effects, and interaction effects using Eqs. (2) and (3). The obtained regression equations in Table 5 are given in terms of the uncoded variables. The regression terms in the ANOVA results for the two parameters (Y_1 and Y_2) showed significant ($P < 0.05$) response surface models with high R^2 and R^2_{adj} values. The R^2 value indicates how much of the variability in the data was accounted for by the model, while the R^2_{adj} value is an R^2 value modified by taking into account the number of covariates or predictors in the model [12,19]. A high confidence is observed when comparing the R^2 and R^2_{adj} values in Table 5, indicating a good fit to the experimental results. The “lack-of-fit” F - and P -values show that the lack of fit is not significant relative to the pure error. Generally, a large F -value and a small P -value for the lack of fit do not result from noise. These models demonstrate that SMX and TOC removal increase with the TiO₂/HAP dose (X_2) and irradiation intensity (X_3) but decrease with SMX concentration (X_1). For the SMX removal, the linear term for X_1 was excluded as insignificant. Interaction effects between the SMX concentration and irradiation inten-

Table 4. ANOVA of the regression parameters of the predicted model for SMX and TOC degradation

Regression	DF	Sum of squares	Mean square	F-value	P-value
Y_1 (SMX removal, %)					
Regression	9	105.465	11.718	110.03	<0.001
Linear	3	94.078	31.359	294.45	<0.001
Quadratic	3	7.182	2.394	22.48	0.002
Crossproduct	3	4.205	1.402	13.16	0.008
Lack of fit	3	0.453	0.1508	3.77	0.217
Y_2 (TOC removal, %)					
Regression	9	145.805	16.201	125.75	<0.001
Linear	3	126.343	42.114	326.89	<0.001
Quadratic	3	8.438	2.813	21.83	0.003
Crossproduct	3	11.025	3.675	28.53	0.001
Lack of fit	3	0.518	0.173	2.72	0.280

Table 5. Regression equations obtained for SMX (Y₁, %) and TOC removal (Y₂, %)

Regression equations
Analysis in coded factor (X ₁ , X ₂ , X ₃)
Y ₁ =95.60+0.19X ₁ +2.14X ₂ +2.68X ₃ -1.33X ₁ ² -0.48X ₂ ² -0.35X ₃ ² -0.73X ₁ X ₃ +0.73X ₂ X ₃ (R ² =99.5%, R ² _{adj} =98.6%)
Y ₂ =45.57+0.56X ₁ +2.50X ₂ +3.04X ₃ -1.36X ₁ ² +0.22X ₂ ² -0.66X ₃ ² +0.63X ₁ X ₂ -1.10X ₁ X ₃ +1.08X ₂ X ₃ (R ² =99.6%, R ² _{adj} =98.8%)
Analysis in uncoded factor (X ₁ , X ₂ , X ₃)
Y ₁ =77.00+1.39X ₁ +5.18X ₂ +0.68X ₃ -0.05X ₁ ² -1.90X ₂ ² -0.01X ₃ ² -0.02X ₁ X ₃ +0.24X ₂ X ₃ (R ² =99.5%, R ² _{adj} =98.6%)
Y ₂ =28.57+1.39X ₁ -3.53X ₂ +0.95X ₃ -0.05X ₁ ² +0.87X ₂ ² -0.02X ₃ ² +0.25X ₁ X ₂ -0.04X ₁ X ₃ +0.36X ₂ X ₃ (R ² =99.6%, R ² _{adj} =98.8%)

sity (X₁X₃) and between the TiO₂/HAP dose and UV intensity (X₂X₃) were observed. The behavior of the process can be described by the *P*-values. On the other hand, for the TOC removal, interaction effects were observed between all terms: for SMX concentration and TiO₂/HAP dose (X₁X₂), SMX concentration and UV intensity

(X₁X₃), and TiO₂/HAP dose and UV intensity (X₂X₃). However, the coefficient of the X₁X₃ term shows that this interaction has adverse effects on SMX and TOC removal (regression constant<0). These results demonstrate that the proposed model is suitable for predicting the amount of SMX and TOC degradation and exhibits rea-

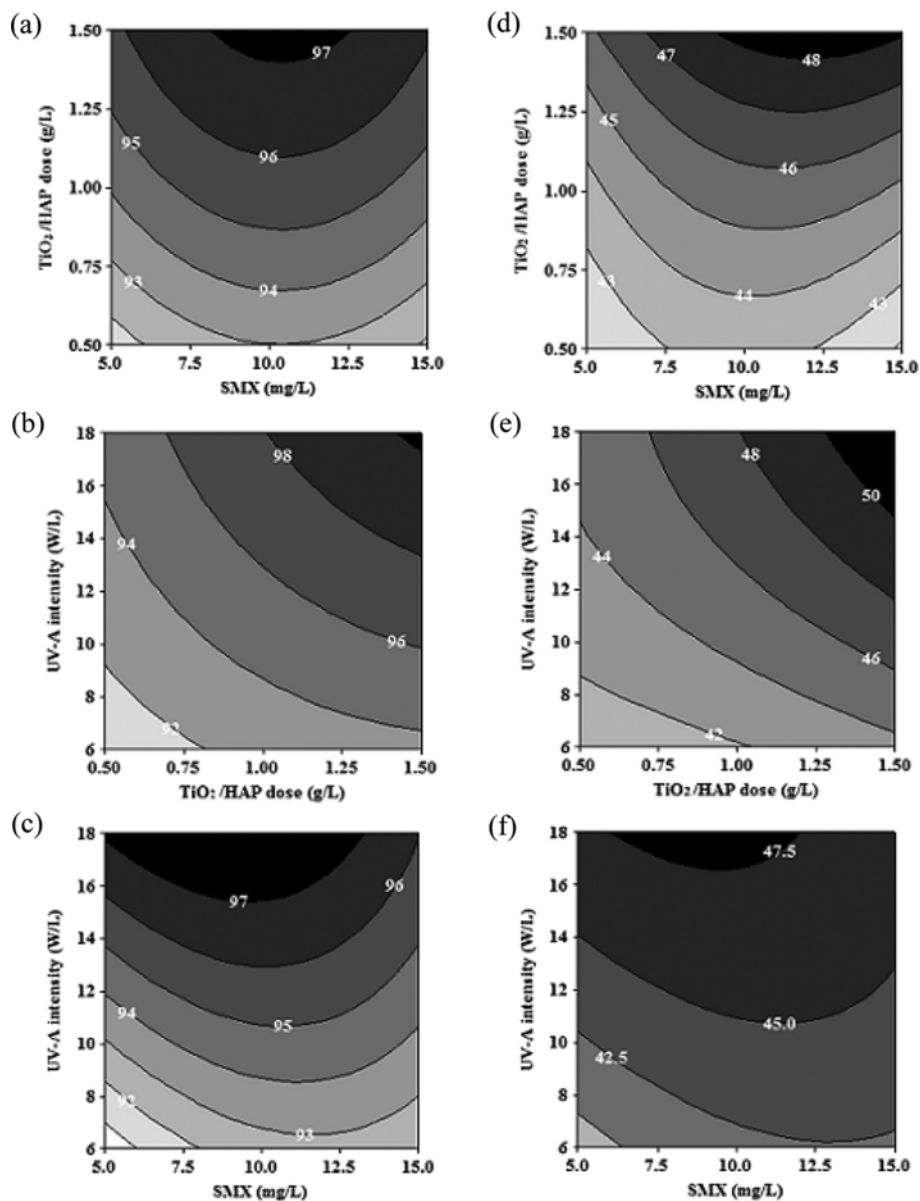


Fig. 3. Contour plots for SMX removal ((a), (c), and (e)) and TOC removal ((b), (d), and (f)). (a), (d) TiO₂/HAP dose with SMX concentration. (b), (e) UV-A intensity with TiO₂/HAP dose. (c), (f) UV-A intensity with SMX concentration.

sonably good agreement with observed results. In particular, the two proposed models were statistically significant, and the observed and predicted results agreed well.

4. Optimization

The optimization and the modeling of the UV-A/TiO₂/HAP system for SMX removal were performed using BBD. The high correlation in the model indicates that the second-order regression equation could be used to optimize the UV-A/TiO₂/HAP system.

Contour plots for the predicted responses were constructed based on the polynomial equation to assess the change in the response results, as shown in Fig. 3. The relationships among the three parameters can also be further understood from these contour plots.

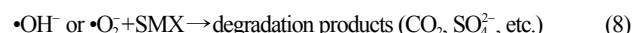
At first, Fig. 3(a) and (d) describe the effects of SMX concentration (X₁) and TiO₂/HAP dose on the different responses. This contour plot shows that the TiO₂/HAP dose (X₂) had a more significant effect on SMX removal than the SMX concentration (X₁). However, the SMX concentration also significantly affected the removal efficiency, as shown in the results of the regression analysis with ANOVA (Table 4 and 5). A similar result was reported by Nasuhoglu et al., who found that decreases in SMX concentration led more degradation of SMX.

Next, the effects of UV intensity (X₃) and TiO₂/HAP dose (X₂) are shown in Fig. 3(b) and (e) for a constant SMX concentration (X₁) at the center point (10 mg L⁻¹). The SMX and TOC removal rate initially increased with increasing of TiO₂/HAP dose and UV-A intensity (Fig. 3(b) and (e)). More than 95% SMX removal (Y₁) was attained at a TiO₂/HAP dose (X₂) of 0.88-1.5 g L⁻¹. As shown in Fig. 3(b), the increase in TiO₂/HAP dose (X₂) combined with the increase in UV intensity (X₃) increased the amount of SMX and TOC removal within the tested ranges of SMX concentration (10 mg L⁻¹). This finding agrees with the results that the removal efficiency increases with increasing of TiO₂/HAP dose. However, according to the results of Hermann's study, an excessive catalyst concentration may decrease the degradation efficiency due to increased light reflectance on the catalyst surface or increased turbidity [18].

The effect of the SMX concentration (X₁) and UV intensity (X₃) at the center-point SMX concentration (X₁) of 10 mg L⁻¹ is also shown in Fig. 3(c) and (f), which shows that the response was dominantly affected by the UV intensity. On the other hand, at a low UV intensity,

the SMX concentration did not significantly affect the SMX or TOC removal.

Therefore, the effects of the TiO₂/HAP dose and UV intensity on the removal efficiency are similar for both SMX and TOC removal: the removal efficiency increased linearly with catalyst dose and UV intensity. Furthermore, the most significant interaction is between the TiO₂/HAP dose (X₂) and UV intensity (X₃). According to Sheng et al. [25], HAP can photodegrade the target compounds through the photoinduced generation of •OH⁻ radicals and •O₂⁻ radicals from the H₂O on the HAP by excitation under UV irradiation (Eqs. (5)-(7)) [26,27]. These radicals can effectively break down the SMX molecules to intermediates such as CO₂, SO₄²⁻, and other degradation products, as shown in Eq. (8) [25-28].



As shown in Fig. 4(a) and (b), actual value versus predicted value shows the results of real application plotted against the predicted responses. It is observed that there are tendencies in the predicted results of linear regression, and the model explains the experimental range studied adequately. The actual result with fitted regression equation showed a good fit of the model.

The optimal values of the dependent variables (Y₁ and Y₂) in the UV-A/TiO₂/HAP system were determined from canonical and ridge analysis of the response surface using SAS 9.1 software. The optimal conditions for maximum SMX removal (99.83%) and TOC removal (49.32%) were an SMX concentration of 5.4145 mg L⁻¹ (X₁), a TiO₂/HAP composite dose of 1.4351 g L⁻¹ (X₂), and an irradiation intensity of 18 W (X₃). These experimental conditions were actually applied to test the validity of the predicted values. Based on the response surface and desired outcome, the optimum conditions for SMX mineralization was obtained. Under these conditions, the predicted removal efficiencies of SMX and TOC removal were 99.83% and 49.32%. To confirm the accuracy of the models and the optimization, some experimental reproducibility tests were car-

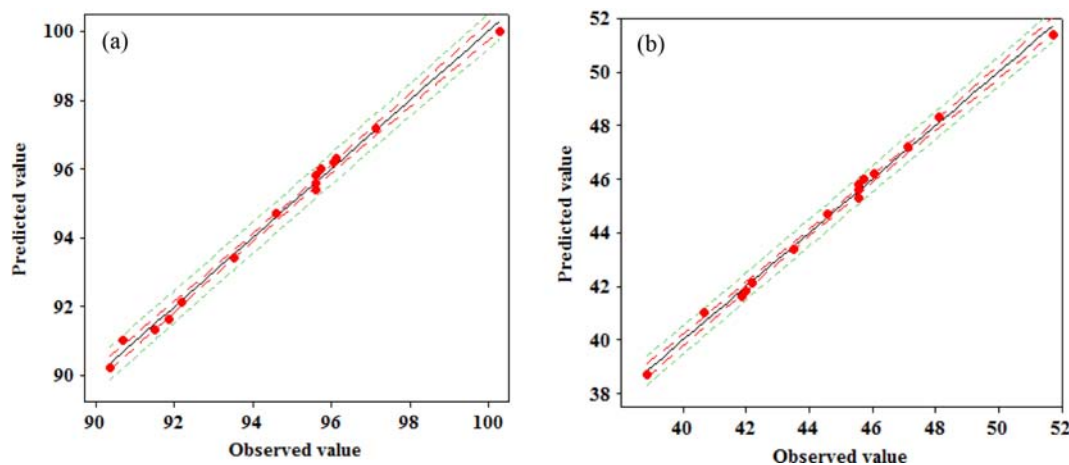


Fig. 4. The observed values (%) plotted against the predicted values (%) derived from the model of SMX (Y₁) and TOC (Y₂) removal in uncoded values for 240 min UV-A irradiation. The regression line with determination coefficient R²=99.5% (a) and 99.6% (b).

Table 6. comparison of actual and predicted value at the optimum condition for three trials of additional experiments

Response	Optimum condition	Predicted value (%)	Observed value (%)
SMX removal (Y ₁)	X ₁ =5.4145 mg L ⁻¹	99.83	99.89±1.20
TOC removal (Y ₂)	X ₂ =1.4351 g L ⁻¹	49.32	51.01±2.61
	X ₃ =18 W L ⁻¹		

ried out under the optimized conditions. In Table 6, the experimental results were found to be in good agreement with the model predictions, with mean SMX and TOC removal of 99.89% and 51.01%, respectively. These results confirm that BBD is effective for analyzing the effects of various parameters and for process optimization for systems such as the UV-A/TiO₂/HAP system for SMX degradation.

CONCLUSION

This study focused on optimizing the process for SMX degradation by a TiO₂/HAP composite with UV-A irradiation. The results obtained are as follows:

1) The TiO₂/HAP composite successfully decomposed nearly 100% of the SMX and mineralized about 50%. The photocatalytic activity of the TiO₂/HAP composite is higher than that of the Degussa P25 TiO₂ because of the synergistic effect between TiO₂ and HAP. The enhanced photocatalytic activity was analyzed using a *Langmuir-Hinshelwood* kinetic model, which showed that the $k_{\text{photocatalysis+adsorption}}$ ($k_p K$) was higher for the composite than for Degussa P25 TiO₂.

2) BBD (regression model and ANOVA) was used to compare quantitatively the main effects and interaction effects of three independent variables. The ensuing mathematical model could predict the amount of SMX removal in any tested range of the experimental conditions and determine the optimal conditions, as well. The high correlation in the model indicates that the second-order polynomial model could be used to determine the effect of each parameter and to optimize the photocatalytic degradation of SMX.

3) In addition, the UV/TiO₂/HAP system was optimized to maximize the SMX removal and mineralization. The SMX concentration (X₁), TiO₂/HAP dose (X₂), and UV intensity (X₃) that maximized the response were 5.4145 mg L⁻¹, 1.4351 g L⁻¹, and 18 W, respectively. Under the optimum conditions, the SMX and TOC removal achieved was 99.89% and 51.01% by actual application. Hence, the TiO₂/HAP composite is recommended as an effective system for SMX degradation.

The TiO₂/HAP composite exhibits enhanced photocatalytic activity. The added HAP decreased the time required for complete degradation of SMX compared with that needed with Degussa P25 TiO₂. As for the optimization procedure, RSM was appropriate for optimizing the operation conditions to maximize the SMX removal of the TiO₂/HAP/UV-A system. However, several other parameters must be considered for actual applications of the UV/TiO₂/HAP system, such as the pH, alkalinity, and scavengers from surface water, which would have various effects on the treatment system.

ACKNOWLEDGEMENTS

This subject is supported by Korea Ministry of Environment as

“Global Top Project” (Project No: GT-11-B2-008-3).

REFERENCES

1. D. Nasuhoglu, V. Yargeau and D. Berk, *J. Hazard. Mater.*, **186**, 67 (2011).
2. T. Herberer, *J. Hydrol.*, **266**, 175 (2002).
3. P. E. Stackelberg, E. T. Furlong, M. T. Meyer, S. D. Zaugg, A. K. Henderson and D. B. Reissman, *Sci. Total Environ.*, **329**, 99 (2004).
4. R. Alexy, T. Kumpel and D. K. Kümmerer, *Chemosphere*, **57**, 505 (2004).
5. J. Azéma, B. Guidetti, A. Korolyov, R. Kiss, C. Roques, P. Constant, M. Daffè and M. Malet-Martino, *European J. Med. Chem.*, **46**, 6025 (2011).
6. S. E. Jørgensen and B. Halling-Sørensen, *Chemosphere*, **40**, 691 (2000).
7. L. Hu, P. M. Flanders, P. L. Miller and T. J. Strathmann, *Water Res.*, **41**, 2612 (2007).
8. M. Tsukada, M. Wakamura, N. Yoshida and T. Watanabe, *J. Mol. Catal. A: Chem.*, **338**, 18 (2011).
9. M. Pratap Reddy, A. Venugopal and M. Subrahmanyam, *Water Res.*, **41**, 379 (2007).
10. R. A. Palominos, A. Mora, M. A. Mondaca, M. Pérez-Moya and H. D. Mansilla, *J. Hazard. Mater.*, **158**, 460 (2008).
11. A. Kumar, B. Prasad and I. M. Mishra, *J. Hazard. Mater.*, **150**, 174 (2008).
12. I.-H. Cho and K.-D. Zoh, *Dyes and Pigments*, **75**, 533 (2007).
13. S. Pushpakanth, B. Srinivasan, B. Sreedhar and T. P. Sastry, *Mater. Chem. Phys.*, **107**, 492 (2008).
14. J. Wang, C. Li, X. Luan, J. Li, B. Wang, L. Zhang, R. Xu and X. Zhang, *J. Mol. Catal. A: Chem.*, **320**, 62 (2010).
15. L. Xu, G. Wang, F. Ma, Y. Zhao, N. Lu, Y. Guo and X. Yang, *Appl. Surf. Sci.*, **258**, 7039 (2012).
16. N. Ma, Y. Zhang and X. Quan, *Water Res.*, **44**, 6104 (2010).
17. N. P. Xekoukoulotakis, C. Drosou, C. Brebou, E. Chatzisyneon, E. Hapeshi, D. Fatta-Kassinos and D. Mantzavinos, *Catal. Today*, **161**, 163 (2011).
18. J. M. Herrmann, J. Didier, P. Pichat, S. Malato and S. Blanco, *Appl. Catal. B: Environ.*, **17**, 15 (1998).
19. E. Kusvuran, S. Irmak, H. I. Yavuz, A. Samil and O. Erbatur, *J. Hazard. Mater.*, **119**, 109 (2005).
20. M. N. Abellán, J. Giménez and S. Esplugas, *Catal. Today*, **144**, 131 (2009).
21. O. González, C. Sans and S. Esplugas, *J. Hazard. Mater.*, **146**, 459 (2007).
22. M. Ahmaruzzaman and D. K. Sharma, *J. Colloid Interface Sci.*, **287**, 14 (2005).
23. K. Lina, J. Pana, Y. Chena, R. Chenga and X. Xua, *J. Hazard. Mater.*, **161**, 231 (2009).
24. Y. Liu, C. Y. Liu, J. H. Wei, R. Xiong, C. X. Pan and J. Shi, *Appl. Surf. Sci.*, **256**, 6390 (2010).
25. Sheng, G, Qiao, L. and Mou, Y., *J. Environ. Eng.*, **137**, 611 (2011).
26. K. Hiroyoshi, L. Masami, M. Yasuyuki and J. B. Moffat, *J. Mol. Catal. A: Chem.*, **252**, 181 (2006).
27. H. Nishikawa, *J. Mol. Catal. A: Chem.*, **206**, 331 (2003).
28. M. P. Reddy, A. Venugopal and M. Subrahmanyam, *Appl. Catal. B*, **69**, 164 (2007).